Shear-flow-induced distortion of the structure of a fluid: Application of a simple kinetic equation

J. F. Schwarzl and S. Hess
Institut für Theoretische Physik, Technische Universität Berlin (PN 7-1), D-1000 Berlin 12, West Germany
(Received 2 December 1985)

The structure of a fluid subjected to a plane Couette flow is calculated starting from a simple model kinetic equation. After the presentation of the general formal solution of this kinetic equation, an expansion in powers of the shear rate is investigated in detail; terms up to order 6 are taken into account. As a specific example, the shear-flow-induced distortion of the structure is analyzed and displayed graphically in the vicinity of its first peak. The pertinent equilibrium structure was chosen to correspond to a soft-sphere fluid where computer simulation data are available for the radial distribution function. Two distinct scattering geometries are considered.

INTRODUCTION

The structure of a "simple" fluid subjected to a shear flow is not simple. In the nonequilibrium situation, the pair-correlation function $g(\mathbf{r})$ and the pertaining structure function $S(\mathbf{k})$ become anisotropic, i.e., they depend not only on the magnitudes of the position vector $\mathbf{r}$ joining a pair of particles or the scattering wave vector $\mathbf{k}$ but also on the directions of these vectors relative to the flow geometry. The distortion of the pair-correlation function linear in the applied shear rate plays a crucial role in the kinetic theory for the viscosity of liquids.[1-4] Nonequilibrium molecular dynamics simulations[5] also show the importance of effects nonlinear in the shear rate.[6-10] Similar remarks apply to model liquids of strongly interacting spherical colloidal particles where the shear-flow-induced distortion of the structure has been measured by light scattering techniques.[11,12]

In this paper, the structure of a fluid subjected to a plane Couette flow is calculated starting from a simple kinetic model equation for the pair-correlation function. This equation has recently been tested in nonequilibrium molecular dynamics simulations.[10,13] Previous theoretical work concerned with the same problem was based on an approximate solution[14] of the Kirkwood-Smolochowski equation; an alternative approach has been put forward more recently.[15] The close similarity between data inferred from computer simulations for soft spheres of Ref. 8 and the light scattering experiments with colloidal solutions[16] deserves particular mentioning.

This paper proceeds as follows. In Sec. I, some general properties of a kinetic equation for the pair-correlation function are discussed and the model assumptions are introduced. A spatial Fourier transformation leads to the corresponding equation for the structure factor. The formal solution of the kinetic equation is presented in Sec. II. For a given equilibrium structure, the shear-flow-induced distortion can be calculated from a power-series expansion in the distortion parameter $\gamma\tau$ where γ is the (constant) shear rate and τ is a configurational relaxation time. Section III is devoted to the choice of a particular equilibrium structure which is inferred from radial distribution of a soft-sphere fluid. Results for the distortion of the structure are then presented in Sec. IV. After some general remarks, the first-order effect (linear in $\gamma\tau$) is discussed. Then the consequences of the higher-order terms are studied for two special scattering geometries, viz., the incident beam parallel to the z and the y directions, respectively, where the flow velocity is in the x direction and its gradient in the y direction. In lowest nonvanishing order in the shear rate γ, the Debye-Scherrer rings experience an elliptical distortion and higher-order terms lead to an intensity modulation around the deformed rings. In the analysis performed, terms up to sixth order in $\gamma\tau$ are included. This approximation seems to be sufficient for $\gamma\tau \lesssim 0.15$ where nonlinear effects can already be noticed clearly. Several graphs are presented which show the distortion of the structure in the vicinity of the first peak for various directions of the scattering wave vector.

I. THE KINETIC MODEL EQUATION

The pair-correlation function $g=g(t,\mathbf{r})$ of a fluid in nonequilibrium subjected to a viscous flow is assumed to obey a kinetic equation of the form[1-4,17]

$$\frac{\partial}{\partial t}g+(\nabla_\mu v_\nu)r_\mu\frac{\partial}{\partial r_\nu}g+D(g)=0\ . \tag{1}$$

Here $\mathbf{r}=\mathbf{r}^{(1)}-\mathbf{r}^{(2)}$ is the difference between the position vectors of two particles 1 and 2 whose relative average velocity $\mathbf{v}^{(1)}-\mathbf{v}^{(2)}$ is approximately by $\mathbf{r}\cdot(\nabla\mathbf{v})$, where $\nabla\mathbf{v}$ is the (constant) gradient of the average-flow velocity field $\mathbf{v}$. In (1), Greek subscripts refer to Cartesian components. For a plane Couette flow in the x direction with the constant velocity gradient (shear rate) γ in the y direction, the flow term of (1) reduces to

$$\gamma r_y\frac{\partial}{\partial r_x}\ .$$

The damping term $D(g)$ guarantees that g approaches its equilibrium value g_{eq} (radial distribution function) in the absence of any external disturbance. It has the general properties

$$D(g_{eq})=0 \tag{2}$$

and

$$\int D(g)d^3r=0 \tag{3}$$

associated with the existence of a thermal equilibrium state and the conservation of the normalization of $g(r)$, respectively. Even the linearized damping term derived from the hierarchy equations with the Kirkwood closure condition for the three-particle correlation is far more complicated[4,17] than the Smoluchowski-type damping term originally proposed by Kirkwood.[1]

Thus, in order to emphasize the effects caused by the flow term of Eq. (1), the damping term is approximated by the simplest ansatz which fulfills conditions (2) and (3), viz.,

$$D(g)=\tau^{-1}(g-g_{eq}) , \tag{4}$$

where $\tau>0$ is a relaxation time. The single relaxation-time approximation (4) can be extended to an ansatz involving a discrete set of relaxation times,[10,13] this extension, however, is not discussed here for the sake of simplicity. With g decomposed as

$$g=g_{eq}+\delta g , \tag{5}$$

where δg is the deviation of g from its equilibrium value, the kinetic model equation (1), for the special geometry and the approximation (4), reduces to

$$\frac{\partial}{\partial t}\delta g+\gamma r_y\frac{\partial}{\partial r_x}\delta g+\tau^{-1}\delta g=-F ,$$

where (6)

$$F=\gamma r_y\frac{\partial}{\partial r_x}g_{eq} .$$

This is an inhomogeneous equation for δg which can be solved for a given equilibrium radial distribution function g_{eq}.

The structure factor $S(\mathbf{k})$, defined by

$$S(\mathbf{k})=1+n\int d^3r(g-1)e^{i\mathbf{k}\cdot\mathbf{r}} , \tag{7}$$

can be decomposed in a way analogous to (5), viz.,

$$S=S_{eq}+\delta S , \tag{8}$$

where S_{eq} is the equilibrium structure factor and δS describes the deviation from equilibrium. In (7), n is the number density. Since δS is essentially the spatial Fourier transform of δg, Eq. (6) leads to a corresponding equation for δS, viz.,

$$\begin{aligned}&\frac{\partial}{\partial t}\delta S-\gamma k_x\frac{\partial}{\partial k_y}\delta S+\tau^{-1}\delta S=-\widetilde{F} ,\\ &\widetilde{F}=-\gamma k_x\frac{\partial}{\partial k_y}S_{eq} .\end{aligned} \tag{9}$$

This inhomogeneous equation for δS can be solved for a given equilibrium structure factor S_{eq}. For the application of a similar kinetic equation but with a diffusionlike damping term to the viscosity problem, see Ref. 18.

II. FORMAL SOLUTION

For a constant shear rate γ and with δg given at $t=0$, the solution of the model kinetic equation (6) can be written as

$$\begin{aligned}g(r_x,r_y,r_z,t)=&e^{-t/\tau}\delta g(r_x-\gamma r_y t,r_y,r_z,0)\\ &-\int_0^t e^{-(t-t')/\tau}\\ &\times F(r_x-\gamma r_y(t-t'),r_y,r_z)dt' .\end{aligned} \tag{10}$$

The stationary solution g_{stat} of g is obtained for $t\gg\tau$ $(t\to\infty)$,

$$\begin{aligned}g_{stat}(r_x,r_y,r_z)=&g_{eq}(r_x r_y,r_z)\\ &-\int_0^\infty dt\, e^{-t/\tau}F(r_x-\gamma r_y t,r_y,r_z) .\end{aligned} \tag{11}$$

Use of the explicit meaning of the quantity F [see (6)] and an integration by parts leads to

$$g_{stat}(r_x,r_y,r_z)=\int_0^\infty d\alpha\, e^{-\alpha}g_{eq}(r_x-\alpha\gamma\tau r_y,r_y,r_z) . \tag{12}$$

Provided that the integrand of (12) can be expanded in powers of the shear rate γ, one obtains the series expansion

$$g_{stat}=g_{eq}-\gamma\tau g^{(1)}+(\gamma\tau)^2g^{(2)}-(\gamma\tau)^3g^{(3)}\cdots , \tag{13}$$

with

$$g^{(j)}=(r_y)^j\frac{\partial^j}{\partial r_x^j}q_{eq} . \tag{14}$$

This expansion is formally equivalent to

$$g_{stat}=\left[1+\gamma\tau r_y\frac{\partial}{\partial r_x}\right]^{-1}g_{eq} . \tag{15}$$

Similarly, the kinetic equation (9) leads to a stationary solution analogous to (12), viz.,

$$S_{stat}(k_x,k_y,k_z)=\int_0^\infty d\alpha\, e^{-\alpha}S_{eq}(k_x,k_y+\alpha\gamma\tau k_x,k_z) . \tag{16}$$

The expressions analogous to (13)—(15) are

$$S_{stat}=S_{eq}+\gamma\tau S^{(1)}+(\gamma\tau)^2S^{(2)}+(\gamma\tau)^3S^{(3)}+\cdots , \tag{17}$$

with

$$S^{(j)}=k_x^j\frac{\partial^j}{\partial k_y^j}S_{eq} , \tag{18}$$

and

$$S_{stat}=\left[1-\gamma\tau k_x\frac{\partial}{\partial k_y}\right]^{-1}S_{eq} . \tag{19}$$

Since for a fluid of spherical particles S_{eq} depends on $\mathbf{k}$ only via $\mathbf{k}^2$, the quantities $S^{(j)}$ defined by (18) can be written as

$$
\begin{aligned}
S^{(1)} &= k_x k_y k^{-2} F_1 , \\
S^{(2)} &= k_x^2 k_y^2 k^{-4} F_2 + k_x^2 k^{-2} F_1 , \\
S^{(3)} &= k_x^3 k_y^3 k^{-6} F_3 + 3 k_x^3 k_y k^{-4} F_2 . \\
S^{(4)} &= k_s^4 k_y^4 k^{-8} F_4 + 6 k_x^4 k_y^2 k^{-6} F_3 + 3 k_x^4 k^{-4} F_2 .
\end{aligned} \tag{20}
$$

The quantities F_j depending on the magnitude k of $\mathbf{k}$ only are given by

$$F_j = k^{2j} \left\{ k^{-1} \frac{d}{dk} \left[k^{-1} \frac{d}{dk} \cdots \left[k^{-1} \frac{d}{dk} S_{\mathrm{eq}} \right] \cdots \right] \right\} , \tag{21}$$

where it is understood that the operation $k^{-1} d/dk$ is performed j times. The expansion (17) with (20) and (21) is used next to evaluate the shear-flow-induced distortion of the structure factor for a special equilibrium structure based on a specifically chosen radial distribution function.

Incidentally, the "Stokes-Maxwell relation" as discussed by Ashurst and Hoover[5] for $g(\mathbf{r})$ and by Clark and Ackerson for $S(\mathbf{k})$ corresponds to the expressions (12) and (16), respectively, if the integrals are replaced by the integrand with $\alpha = 1$. The terms linear in $\gamma\tau$ resulting from this approximation coincide with the linear terms of (13) and (17).

III. RADIAL DISTRIBUTION AND EQUILIBRIUM STRUCTURE

In view of the wealth of data available for the "soft-sphere computer fluid" and its relevance for colloidal model fluids,[16,19] it was decided to use, as a specific example, an analytic expression for the radial distribution function which matches $g_{\mathrm{eq}}(r)$ of the soft-sphere fluid with a r^{-12} potential at a temperature $T = 0.25$ and the density $n = 0.7$. The quantities T and n are in reduced units,[8–10] and the density where the fluid coexists with the solid phase[20] is $n \approx 0.82$. On the other hand, it is desirable to represent $g_{\mathrm{eq}}(r)$ in a functional form where the Fourier transformation (7) required to obtain the equilibrium structure function $S_{\mathrm{eq}}(k)$ can be performed analytically.

The ansatz chosen was

$$g_{\mathrm{eq}}(r) = \sum_{i=0}^{I} f_i(r) , \tag{22}$$

with

$$f_0(r) = 1 - \exp[-(\eta_0 r)^{2N_0}] , \tag{23}$$

and

$$f_i(r) = b_i r^{2N_i} \exp(-\eta_i r^2), \quad i \geq 1 . \tag{24}$$

In this representation, g_{eq} is an even function of r which vanishes for $r = 0$ and approaches the value 1 for $r \to \infty$. The term f_0 is a nearly steplike function which increases from 0 to 1 at about $r = 1/\eta_0$. This increases is steeper the larger the parameter N_0 is. The terms (24) should mimic the maxima and minima of g_{eq}. In particular, f_i, $i \geq 1$, possesses an extremum at $r = X_i$, with its extremal value $M_i = f_i(X_i)$. The parameter N_i is a measure for the width of the peak or of the dip. These values are related to each other by

$$\eta_i = N_i X_i^{-2}, \quad b_i = M_i (e^{1/2} X_i^{-1})^{2N_i} . \tag{25}$$

The parameters occurring in (23) and (24) are chosen such that (22) is a reasonable approximation for the function g_{eq} of a fluid of particles interacting with the potential $\Phi = r^{-12}$ at the state point mentioned above over the range $r = 0.8$–2.5 where data are available from a molecular dynamics calculation.[8] As restrictions on the parameters, it is required that (22) yields the correct potential contribution to the pressure

$$P^{\mathrm{pot}} = 8\pi n^2 \int_0^\infty r^{-10} g_{\mathrm{eq}}(r) dr , \tag{26}$$

where P^{pot} is known from the simulation. Furthermore, the "canonical" normalization

$$4\pi n \int_0^\infty r^2 (g_{\mathrm{eq}} - 1) dr = -1 \tag{27}$$

is imposed for simplicity rather than the "grand-canonical" normalization which links the integral on the left-hand side of Eq. (27) with the compressibility. Since the compressibility is small, the relation (27) is a good approximation for the present system.[16] The actual choice of the parameters occurring in (22)–(25) can be inferred from Table I; here it suffices to mention that just seven terms ($I = 6$) are included in the sum (22). In Fig. 1, the comparison of the analytic approximation for g_{eq} with the computer data is displayed; Fig. 2 shows g_{eq} and $r^2(g_{\mathrm{eq}} - 1)$ over a somewhat larger range of r values.

The Fourier transformation of (22), according to (7), yields the equilibrium structure function

$$S_{\mathrm{eq}} = 1 + \sum_{i=0}^{I} S_i , \tag{28}$$

with

$$S_0 = 4\pi n \int_0^\infty [f_0(r) - 1] r^2 \frac{\sin(kr)}{r} dr , \tag{29}$$

and

$$S_i = 4\pi n \int_0^\infty f_i(r) r^2 \frac{\sin(kr)}{r} dr, \quad i \geq 1 . \tag{30}$$

Here k is the magnitude of the wave vector $\mathbf{k}$. Use has been made of the fact that g_{eq} is an isotropic function. The expression (23) for f_0 leads to

$$S_0 = 4\pi n \eta_0^{-3} \sum_{l=0}^{\infty} B_l (k \eta_0^{-1})^{2l} , \tag{31}$$

TABLE I. Parameters occurring in Eqs. (22)–(25) used for the approximation to the radial distribution function.

$I = 6$	$\eta_0 = 0.981$	$N_0 = 30$
$M_1 = 1.48$	$X_1 = 1.145$	$N_1 = 82$
$M_2 = 0.35$	$X_2 = 1.3$	$N_2 = 60$
$M_3 = -0.35$	$X_3 = 1.69$	$N_3 = 30$
$M_4 = 0.31$	$X_4 = 2.2$	$N_4 = 80$
$M_5 = -0.12$	$X_5 = 2.7$	$N_5 = 60$
$M_6 = 0.020\,19$	$X_6 = 3.2$	$N_6 = 60$

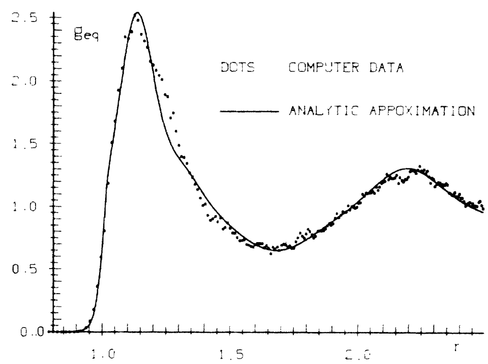

FIG. 1. Analytical approximation for the radial distribution function g_{eq}; comparison with the computer data.

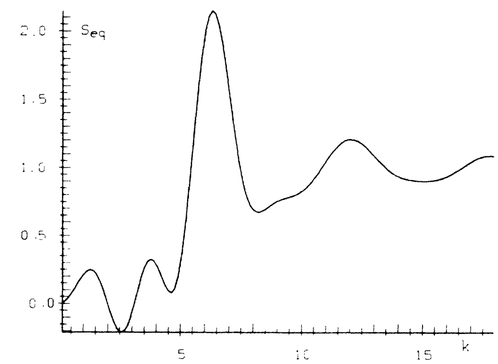

FIG. 3. Equilibrium structure factors S_{eq} as function of the magnitude of the scattering wave vector k.

with the coefficients B_l given by

$$B_l=(-1)^{l+1}(2l+3)^{-1}\Gamma\left[1+\frac{2l+3}{2N_0}\right]\Big/\Gamma(2l+2)\ . \quad (32)$$

The series (31) converges fast for all $k\eta_0^{-1}$. Similarly, (30) with (24) yields

$$S_i=nR_ik_i^{-1}\exp(-k_i^2)H_{2N_i+1}(k_i)\ , \quad (33)$$

with

$$k_i=\tfrac{1}{2}k(\eta_i)^{-1/2}\ , \quad (34)$$

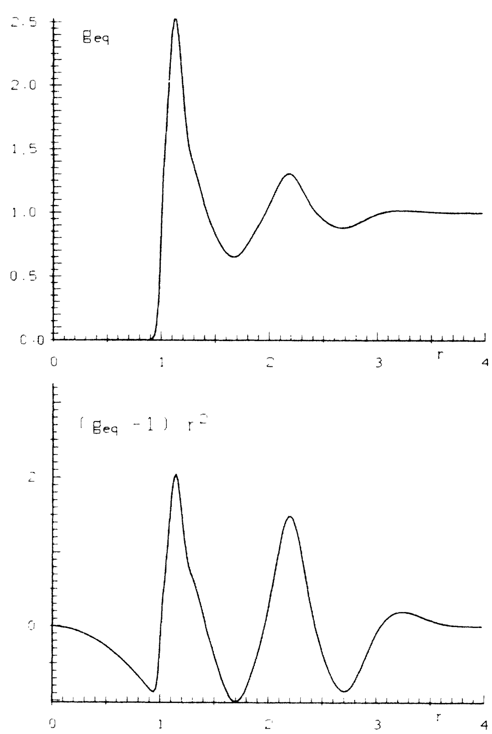

FIG. 2. Radial distribution function (upper picture) and the integrand of the normalization condition [Eq. (27)] (lower picture) as functions of R.

$$R_i=(-1)^{N_i}M_i\frac{\pi^{7/4}}{\sqrt{2}}\left[\frac{e}{2}\right]^{N_i}N_i^{-1}X_i^3\left[\frac{(2N_i+1)!}{N_i^{(2N_i+1)}}\right]^{1/2}\ . \quad (35)$$

The function H_l occurring in (33) is a normalized Hermite polynomial with the property

$$\int_{-\infty}^{+\infty}\exp(-x^2)H_l(x)H_j(x)dx=\delta_{lj}\ . \quad (36)$$

The equilibrium structure S_{eq} resulting from the above given expressions with the same parameters as those underlying the function g_{eq} of Figs. 1 and 2 is displayed in Fig. 3. The oscillations of S_{eq} for $k<5$ are unphysical and result from the fact that g_{eq} is only well determined over a rather small range of r values.

The first peak of S_{eq} occurs at $k=k_{max}\approx 6.3$. The first maximum of g_{eq} is at $r=r_{max}\approx 1.14$; thus one has $k_{max}r_{max}\approx 7.2$. In the following, the main attention is focussed on the distortion of the structure factor in the vicinity of the first peak which is responsible for the most intensive Debye-Scherrer ring in a light scattering experiment.[11,12,16]

IV. DISTORTION OF THE STRUCTURE FACTOR

A. General remarks

The structure factor in the presence of a viscous flow can now be computed from Eqs. (17) and (18) and (20) and (21) for S_{eq} given by (28)–(34). In particular, the functions F_j of (20) can be written as

$$F_j(k)=T_{0,j}+\sum_{i=1}^{I}T_{i,j}\ , \quad (37)$$

where the first index $T_{i,j}$ refers to the labeling of the various terms in (28) and j indicates the order of the operation $k^{-1}d/dk$ as in (21), e.g.,

$$T_{0,1}=k\frac{dS_0}{dk},\quad T_{5,2}=k^4\left[k^{-1}\frac{d}{dk}\left[k^{-1}\frac{dS_5}{dk}\right]\right]\ .$$

The series expansion (31) leads to

$$T_{0,j}=2^{2+j}\frac{\pi n}{\eta_0^3}\sum_{l=j}^{\infty}\frac{l!}{(l-j)!}B_l(k/\eta_0)^{2l}\,. \tag{38}$$

The property

$$(d/dz)[e^{-z^2}H_l(z)]=-2\sqrt{(l+1)/2}e^{-z^2}H_{l+1}(z)$$

of the Hermite polynomials allows the iterative calculation of $T_{i,1}, T_{i,2}, \ldots$ from (33), e.g.,

$$T_{i,1}=-S_i-2nR_i\sqrt{(N_i+1)}e^{-k_i^2}H_{2N_i+2}(k_i)\,; \tag{39}$$

for k_i and R_i see (34) and (35). Some remarks on the distortion of $S(\mathbf{k})$ linear in the shear rate γ are made next.

B. First-order effect

In first order in $\gamma\tau$, the angle dependence of the distorted-structure factor is determined by $k^{-2}k_xk_y$, cf. Eq. (20). It is recalled that $\mathbf{k}=\mathbf{k}_1-\mathbf{k}_0$ is the difference between the wave vectors $\mathbf{k}_0$ and $\mathbf{k}_1$ of the incident and the scattered radiation. For elastic scattering one has $|\mathbf{k}_0|\equiv k_0=|\mathbf{k}_1|$, and $k_0=2\pi/\lambda$ where λ is wavelength. The simplest scattering geometry which allows the detection of the first-order effect is with $\mathbf{k}_0$ parallel to the z direction; for small-angle scattering, $\mathbf{k}$ is then in the shear plane determined by the flow velocity (x direction) and its gradient (y direction). More generally, one has $k=2k_0\sin(\frac{1}{2}\theta_1)$ where θ_1 is the angle between $\mathbf{k}_0$ and $\mathbf{k}_1$, and

$$k^{-2}k_xk_y=\sin^2\theta\sin\varphi\cos\varphi=\tfrac{1}{2}\cos^2(\tfrac{1}{2}\theta_1)\sin(2\varphi)\,. \tag{40}$$

Here θ and φ are the polar angles of k; θ is related to θ_1 by $\theta=\pi/2+\frac{1}{2}\theta_1$. With θ eliminated in favor of k_0, the full first-order distortion is given by

$$\gamma\tau S^{(1)}=\gamma\tau\tfrac{1}{2}\left[1-\left[\frac{k}{2k_0}\right]^2\right]\sin(2\varphi)F_1(k)\,. \tag{41}$$

Clearly, in contradistinction to the equilibrium structure $S_{\rm eq}$, $S=S_{\rm eq}+\gamma\tau S^{(1)}$ not only depends on k but also on the angle φ and on k/k_0. The latter dependence can be ignored for small-angle scattering where $k\ll 2k_0$.

In Fig. 4, the quantity $F_1(k)$ occurring in (41) is displayed together with $S_{\rm eq}$ for the special radial distribution discussed above. The angle dependence as given by

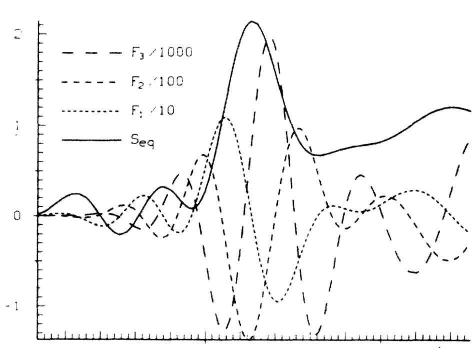

FIG. 4. Graphs of the equilibrium structure $S_{\rm eq}$ and of the first three functions $F_j/10^j$ as used in (20).

(40) yields the strongest distortion of the structure in the shear plane in the directions which form the angles 45° and 135° with the flow direction. From Fig. 4 one infers that in the 45° direction, the peak of $S(\mathbf{k})$ at $k\approx 6$ is shifted towards smaller k values, and at 135° it is shifted to larger k values. The resulting (first-order) elliptical distortion of the Debye-Scherrer rings is the most prominent feature observed in the light scattering experiments.[11,12,16] However, at shear rates γ with $\gamma\tau \gtrsim 10^{-1}$ nonlinear effects also can be noticed.

C. Nonlinear distortion in the shear plane

According to (20), the second-order distortion of $S(\mathbf{k})$ proportional to $(\gamma\tau)^2$ contains two terms with their angle dependence determined by

$$k^{-2}k_x^2\cos^2(\tfrac{1}{2}\theta_1)\cos^2\varphi=[1-(k/2k_0)^2]\cos^2\varphi\,, \tag{42}$$

and

$$k^{-4}k_x^2k_y^2=\tfrac{1}{4}\cos^4(\tfrac{1}{2}\theta_1)\sin^2(2\varphi)$$
$$=\tfrac{1}{4}[1-(k/2k_0)^2]\sin^2(2\varphi)\,. \tag{43}$$

The same scattering geometry as in the preceding subsection is considered. The first term (42), which has to be multiplied by F_1, has its largest effect for $\varphi=0$ and $\varphi=180°$. Since $\cos^2\varphi=\frac{1}{2}[1+\cos(2\varphi)]$, this term implies a rotation of the principal axes of the first-order Debye-Scherrer ellipses away from the 45°, 135° directions by the angle χ determined by

$$\tan(2\chi)=\gamma\tau\,. \tag{44}$$

The term (43) which is multiplied by F_2 has a fourfold symmetry; notice that $\sin^2(2\varphi)=\frac{1}{2}-\frac{1}{2}\cos(4\varphi)$. Since F_2 is negative in the vicinity of the first peak of $S_{\rm eq}$ (cf. Fig. 4), this term leads to an intensity modulation around the elliptical Debye-Scherrer ring with extra intensities at $\varphi=0°$, 90°, 180°, and 270°. This feature, again, is observed in the light scattering experiments.[12,16] The angle dependence of the higher-order terms as given by (20) can be

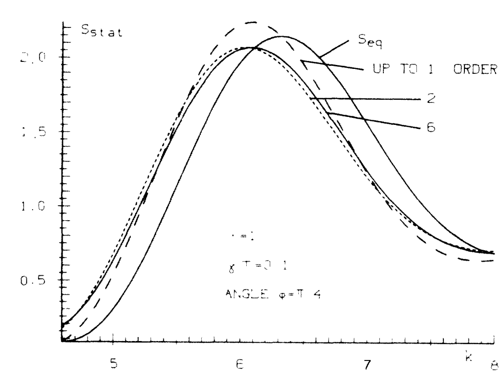

FIG. 5. Structure factor in the vicinity of its maximum for a shear flow with $\gamma\tau=0.1$. Curves are displaced where terms up to the first, second, and sixth orders are taken into account, respectively. Notice that there is little difference between the second- and sixth-order approximations. The equilibrium structure is also shown for comparison.

analyzed in a similar way. Third-order terms, e.g., lead to rotation of the four-fold pattern away from the 0°, 90° directions and to an extra six-fold intensity modulation.

The functions F_j defined by (21) are of crucial importance for the quality of a finite-sum approximation for $S(\mathbf{k})$ as given by (17); here terms up to order 6 are included. In Fig. 5, the undisturbed structure factor 1 in the vicinity of the first peak and for $\varphi=45°$ is compared with the various approximations. The wavelength $\lambda=1$, i.e., $k/2k_0=1/4\pi$, has been chosen. The "distortion parameter" $\gamma\tau$ has the value 0.1. Clearly, the first-order perturbation describes the shift of the peak but overestimates its height. The second-order approximation is already very close to the higher-order approximations. For $\gamma\tau=0.15$, a similar analysis still shows a reasonable convergence of the successive approximations; for $\gamma\tau=0.2$, however, even the sixth-order perturbation is not small compared with the lower-order distortions.

Thus for the specific equilibrium structure considered here, the present model calculations yield meaningful results for $\gamma\tau<0.15$; second-order effects already show up for $\gamma\tau>0.05$. Figure 6 shows the structure factor in the vicinity of the first peak for $\varphi=45°$ and 135°, $\lambda=1$, as evaluated by the series (17) and (20) where terms up to the sixth order are taken into account. The distortion parameter $\gamma\tau$ has the values 0, 0.01, 0.03, 0.05, 0.07, and 0.09. Notice the increasing shift and the broadening of the curves. More specifically, the shift of the first peak in the 45° and 135° directions is linear in $\gamma\tau$ up to $\gamma\tau\approx 0.12$ and approximately given by $\mp 0.4k_m\gamma\tau$, respectively. Here, k_m is the magnitude of the wave vector at the first maximum of the undistorted structure. The above-mentioned results obtained from the numerical analysis is close to the corresponding expression $\mp 0.5k_m\gamma\tau$ which has previously

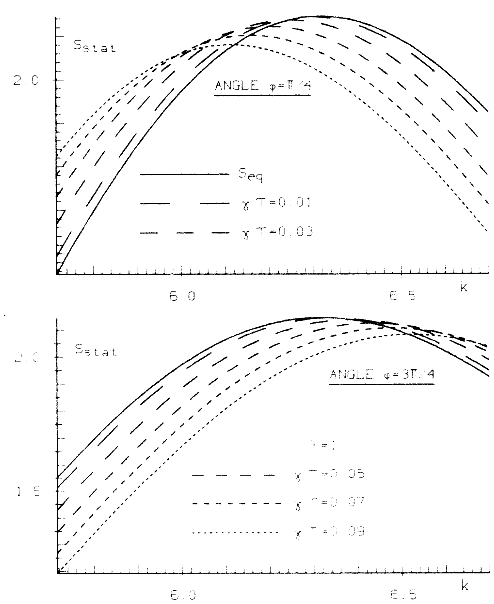

FIG. 6. Structure factors for various values of the distortion parameter $\gamma\tau$. The projection of the scattering wave vector onto the shear plane encloses the angles $\varphi=\pi/4$ (upper picture) and $\varphi=3\pi/4$ (lower picture) with the flow direction.

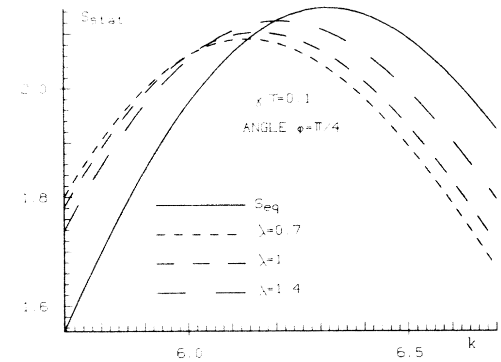

FIG. 7. Distorted structure factor in the vicinity of the first peak for $\gamma\tau=0.1$ and $\varphi=\pi/4$ as in Fig. 6. The various dashed curves are for three different values of the wavelength of the incident beam. Again, the equilibrium structure is shown for comparison.

been inferred from simpler theoretical considerations.[11,12,14]

In Fig. 7, the equilibrium structure is compared with the distorted structure for $\varphi=45°$ and $\gamma\tau=0.1$ with various values chosen for the wavelength λ, in particular $\lambda=0.7$, 1.0, 1.4. Clearly, the distortion is larger for the smaller λ values, i.e., it can be observed more easily in small-angle scattering.

D. Distortion for the incident beam along the gradient direction

An experimental setup where the wave vector $\mathbf{k}_0$ of the incident beam is parallel to the gradient of the velocity field (y direction) is particularly convenient for neutron scattering;[21] light scattering experiments have also been performed for this geometry.[12] For the case of extreme small-angle scattering, $k \ll k_0$, the scattering vector $\mathbf{k}$ is then in the x-z plane, i.e., $k_y=0$. As a consequence, the series (17) with (20) reduces to

$$S=S_{\text{eq}}+(\gamma\tau)^2k_x^2k^{-2}F_1+(\gamma\tau)^4k_x^4k^{-4}F_2+\cdots \quad . \tag{45}$$

Clearly, this is an even function of γ. Notice that the second- and fourth-order terms involve the functions F_1 and F_2 which occur in connection with the first- and second-order terms for the geometry treated in the preceding subsection.

The scattering pattern in the x-z plane resulting from (45) is dominated by the elliptical distortion of the Debye-Scherrer rings; now their principal directions are parallel to the x direction (flow velocity) and the z direction. The fourth-order term of (45) also leads to a four-fold intensity modulation around the distorted ring. Again, these features are observed experimentally.

If the condition $k \ll k_0$ is not fulfilled, all terms of (17) and (20) contribute to the scattering intensity. For the first few terms this is inferred from

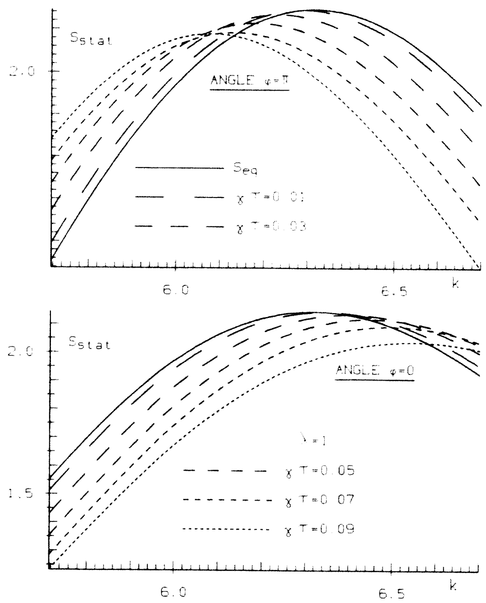

FIG. 8. Distorted structure factor as function of k for the incident beam parallel to the direction of the gradient of the flow velocity. The various curves are for several values of the distortion parameter $\gamma\tau$; the projection of the scattering wave vector onto the plane normal to the incident beam is parallel (upper picture, $\varphi=0$) and antiparallel (lower picture, $\varphi=\pi$) to the flow direction.

$$\begin{aligned} k_x k_y k^{-2} &= -(k/2k_0)[1-(k/2k_0)^2]^{1/2}\cos\varphi_1 \, , \\ k_x^2 k^{-2} &= [1-(k/2k_0)^2]\cos^2\varphi_1 \, , \\ k_x^2 k_y^{-4} &= (k/2k_0)^2[1-(k/2k_0)^2]\cos^2\varphi_1 \, , \end{aligned} \tag{46}$$

where φ_1 is the angle which the projection of $\mathbf{k}$ onto the x-z plane encloses with the x direction. Similar expressions can be obtained for the higher-order terms. In Fig. 8, S_{eq} and the distorted structure for $\varphi_1=0$ and $\varphi_1=180°$ with $\lambda=1$ (i.e., $k/2k_0=1/4\pi$) are plotted for the same values of the distortion parameter $\gamma\tau$ as used for Fig. 6. Again, a shear-induced shift of the first maximum and a decrease of its height and a broadening of the curve are found. Notice that in this geometry the effect is practically as strong as for the previously considered case. The case $\varphi_1=90°$ corresponds to $k_x=0$. Equations (19) and (20) imply that the structure factor is not affected by the shear flow (in all orders in $\gamma\tau$) for this specific direction.

CONCLUDING REMARKS

In this paper, the consequences of a simple model kinetic equation for the shear-flow-induced distortion of the structure have been presented. After the derivation of a general expression for this distortion, it has been analyzed in detail for a fluid with a special equilibrium structure. Two types of scattering geometries were considered explicitly. The importance of terms nonlinear in the shear rate was stressed. The model yields good qualitative agreement with the experimentally observed structure. For a quantitative comparison, however, it would be desirable not only to have contour maps of the scattered intensity but good structure factors for specific directions of the scattering vector—as considered here—or an analysis of the intensity maps which projects out certain angle-dependent parts intimately linked with the expansion of the pair-correlation function used in theoretical work[14] and in computer simulation.[7–10]

Of course, fluids with other equilibrium structures also can be studied by the present approach. An extension of the method to oriented ferrofluids[22] is of interest and seems to be feasible.

[1] J. G. Kirkwood, J. Chem. Phys. **14**, 180 (1946); J. G. Kirkwood, F. B. Buff, and M. S. Green, *ibid.* **17**, 149 (1949).

[2] H. S. Green, *Structure of Liquids,* Vol. 10 of *Handbuch der Physik* (Springer, Berlin, 1960).

[3] R. Eisenschitz, *Statistical Theory of Irreversible Processes* (Oxford University Press, Oxford, 1958).

[4] S. Hess, Physica **118A**, 79 (1983).

[5] W. T. Ashurst and W. G. Hoover, Phys. Rev. A **11**, 658 (1975).

[6] *Nonlinear Flow Behavior,* edited by H. J. M. Hanley (North-Holland, Amsterdam, 1983).

[7] D. J. Evans, Phys. Rev. A **23**, 1988 (1981).

[8] S. Hess and H. J. M. Hanley, Phys. Rev. A **25**, 1801 (1982); Int. J. Thermophys. **4**, 97 (1983).

[9] D. J. Evans, H. J. M. Hanley, and S. Hess, Phys. Today **37** (No. 1), 26 (1984).

[10] S. Hess, J. Phys. (Paris) **46**, C3-191 (1985).

[11] N. A. Clark and B. J. Ackerson, Phys. Rev. Lett. **44**, 1005 (1980).

[12] B. J. Ackerson and N. A. Clark, Physica **118A**, 221 (1983).

[13] S. Hess and H. J. M. Hanley, Phys. Lett. **98A**, 35 (1983).

[14] S. Hess, Phys. Rev. A **22**, 2844 (1980).

[15] D. Ronis, Phys. Rev. Lett. **52**, 473 (1984).

[16] H. J. M. Hanley, J. C. Rainwater, N. A. Clark, and B. J. Ackerson, J. Chem. Phys. **79**, 4448 (1983).

[17] T. Ohtsuki, Physica **108A**, 441 (1981).

[18] J. C. Rainwater and S. Hess, Physica **118A**, 371 (1983).

[19] S. Hess, J. Mec. Theor. Appl., Special Issue, 1985.

[20] W. G. Hoover *et al.*, J. Chem. Phys. **52**, 493 (1970).

[21] J. Hayter, B. J. Ackerson, and N. A. Clark (private communication).

[22] S. Hess, B. J. Hayter, and R. Pynn, Mol. Phys. **53**, 1527 (1984).